Pre-Percutaneous Coronary Intervention Lesion Assessment

6

Sung Yun Lee

6.1 Introduction

Traditionally, quantitative coronary angiography (QCA) was the major imaging modality to assess the severity of CAD for coronary lesion assessment when coronary artery disease is treated with catheter-based coronary interventions. But only provides lumenogram or shadowgram a planar two-dimensional silhouette of the lumen contains only about 25% of the total coronary blood flow and is unsuitable for the precise assessment of atherosclerosis. Intravascular ultrasound (IVUS) provides a unique real-time, tomographic assessment of coronary artery assessment of lesion characteristics, lumen diameters, cross-sectional area, plaque area, and distribution. Generally coronary angiography underestimates the severity and extent of disease, IVUS is golden standard for accurate evaluation for pre-intervention lesion assessment.

Current USA [1] and European guidelines [2] for coronary revascularization recommend IVUS use with class IIa for assessment of angiographically indeterminant left main disease, stent stenosis or failure lesion, stent optimization for selected patients, and evaluation for cardiac allograft vasculopathy (Table 6.1).

Table 6.1 Class IIa recommendation for clinical values of intravascular ultrasound of current coronary revascularization guidelines

2011 ACCF/AHA/SCAI Guideline [1]	Level of evidence
Assessment of angiographically indeterminant left main CAD	B
Reasonable 4–6 weeks and 1 year after cardiac transplantation to exclude donor CAD, detect rapidly progressive cardiac allograft vasculopathy, and provide prognostic information	B
Determine the mechanism of stent restenosis	C
2014 ESC/EACTS guidelines on myocardial revascularization [2]	
Optimize stent implantation in selected patients[a]	B
Assess severity and optimize treatment of unprotected left main lesions	B
Assess mechanism of stent failure	B

[a]In reducing restenosis and adverse events after bare metal stent implantation, better clinical and angiographic results may be obtained under IVUS guidance

6.2 Angiographic Indeterminant Non-Left Main Coronary Artery Stenosis

Fractional flow reserve (FFR; the ratio of distal to proximal pressure at maximum hyperemia) is the standard method for assessing the physiologic significance of a non-left main coronary artery (LMCA) lesion. IVUS has been corrected for vessel size, but IVUS has not been able to factor

S.Y. Lee
Inje University Ilsan Paik Hospital,
Goyang, South Korea
e-mail: im2pci@gmail.com

M.-K. Hong (ed.), *Coronary Imaging and Physiology*,
https://doi.org/10.1007/978-981-10-2787-1_6

in the amount of subtended viable myocardium. IVUS minimal lumen area (MLA) in predicting hemodynamic significance in non-LMCA lesions is that the functional effects of a lesion are dependent on additional factors besides dimension. These include lesion location in the coronary tree, lesion length, eccentricity, entrance and exit angles, shear forces, reference vessel dimensions, and the amount of viable myocardium subtended by the lesion [3].

Therefore, in non-LMCA lesions there is only moderate correlation between anatomic dimensions by IVUS and ischemia by physiological assessment. Many studies have attempted to identify invasive IVUS minimum lumen area (MLA) criteria that are equivalent to FFR, reported IVUS MLA cut-off thresholds range from 2.3 to 3.9 mm^2 (Table 6.2) [4–14].

In earlier study IVUS MLA < 4.0 mm^2 correlates with ischemia on single-photon emission computed tomography and also correlates moderately well with an FFR < 0.75. Importantly, low event rates are observed in intermediate lesions when intervention is deferred with an IVUS MLA ≥ 4 mm^2 [15–17]. In the largest study to date, IVUS was compared with FFR in 544 lesions [13]. The optimal cut-off value for predicting an FFR ≤ 0.80 was an MLA = 2.9 mm^2 by IVUS, but the overall accuracy was only 66%. Moreover, of the 240 lesions that had an MLA < 2.9 mm^2, only 47% was hemodynamically significant by FFR. Similarly concerning, 19% of lesions with an MLA > 2.9 mm^2 had an FFR < 0.80, limiting the utility of IVUS for lesion assessment. Kang et al. [7, 8] evaluated 236 angiographically intermediate coronary lesions in which both IVUS and FFR measurements were performed. An IVUS MLA_2.4 mm^2 had the maximum accuracy for predicting FFR < 0.80. However, the overall diagnostic accuracy was 68% with a confidence interval ranging from 1.8 to 2.6 mm^2. FIRST was a multicenter prospective registry of patients who underwent elective coronary angiography and had intermediate coronary stenosis (40–80%) [12]. An IVUS-measured MLA < 3.07 mm^2 had the best sensitivity and specificity (64% and 64.9%, respectively) for correlating with FFR < 0.80.

So, FFR should be considered the standard for assessing the hemodynamic significance of intermediate non-LMCA lesions and better validated than IVUS as a physiologic assessment. An MLA < 4.0 mm^2 has reasonable accuracy in identifying non-significant lesions for which percutaneous coronary intervention (PCI) can be safely deferred [18]. However, an MLA < 4.0 mm^2 does not accurately predict a hemodynamically significant lesion and should not be used in the absence of supporting functional data (such as DEFER, FAME-I, or FAME-II with FFR) to recommend revascularization [3]. An MLA < 3.0 mm^2 is most likely a significant stenosis, but due to its only modest sensitivity and specificity, physiologic testing is desirable before

Table 6.2 Studies correlating intravascular ultrasound to FFR in non-left main intermediate disease

	Takagi et al [4]	Briguori et al [5]	Lee et al [6]	Kang et al [7, 8]	Ben-Dor et al [9, 10]	Koo et al [11]	Waksman et al [12]	VERDICT/ FIRST [13]	Kang et al [14]
No of lesion	51	53	94	236	205	267	304	544	700 LAD
Angiographic DS %	30–70	40–70	30–75	30–75	40–70	30–70	40–80	40–80	30–75
IVUS mean MLA (mm^2)	3.9	3.9	2.3	2.6	3.5	3.0	3.5	3.0	2.5
IVUS MLA cut-off (mm^2)	4.0	4.0	2.0	2.4	3.1	2.8	3.07	3.0	2.5
Year of publication	1999	2001	2010	2011	2011	2011	2013	2013	2013

FFR fractional flow reserve, *LAD* left anterior descending, *DS* diameter stenosis, *IVUS* intravascular ultrasound, *MLA* minimal lumen area, *A* study with Asian populations

Table 6.3 Studies correlating intravascular ultrasound to FFR to identify functional significant LMCA lesion

	N	FFR cut-off	Route of adenosine	IVUS correlation with FFR	Defer	Survival defer (%)	Revascularization	Survival revascularization (%)
Jasti et al [20]	55	0.75	IC	MLA 5.9 mm^2 MLD 2.8 mm	24	100	20 PCI 11 CABG	100
Park et al [22]	112	0.80	IV	MLA 4.5 mm^2	NA	NA	NA	NA
Kang et al. [23]	55	0.80 0.75	IV	MLA 4.8 mm^2 MLA 4.1 mm^2	25	NA	29 PCI 1 CABG	NA

FFR fractional flow reserve, *LMCA* left main coronary artery, *IC* intracoronary, *IV* intravenous, *MLA* minimal lumen area, *MLD* minimal lumen diameter, *PCI* percutaneous coronary intervention, *CABG* coronary artery bypass graft, *NA* not available

proceeding with revascularization. It may be acceptable to defer an intervention in selected situations based on MLA size, IVUS should never be used to justify an intervention.

6.3 Left Main Coronary Artery Lesion

Left main coronary artery (LMCA) lesion has greatest angiographic assessment variability. Small real-world analysis showed that less than half of intermediate LMCA had significant stenosis by IVUS assessment, especially for lesions located at the left main ostium [19].

IVUS evaluation for LMCA stenosis can be valuable when coronary angiography gives equivocal or ambiguous images. Both IVUS and FFR have theoretical and practical limitations for LMCA lesion, proximal LAD and/or LCX disease can impact FFR of LMCA stenosis. With IVUS, distal LMCA lesions can be difficult to accurately image, and often require pullback from both the LCX and LAD. But limited variability in LMCA length, diameter, and amount of supplied myocardium explains the better correlation in LMCA with FFR than non-LMCA stenosis, the most widely used parameter is MLA in LMCA stenosis.

Jasti et al. [20] showed good correlation between FFR and IVUS, with good sensitivities and specificities >0.90. In a study of 55 intermediate LMCA lesions (reference diameter 4.2 mm), an MLA <5.9 mm^2 and an MLD <2.8 mm correlated well with FFR < 0.75.

A prospective application of these criteria was tested in the LITRO study [21]. LMCA revascularization was performed in 90.5% of patients with an MLA < 6 mm^2 and was deferred in 96% of patients with an MLA > 6 mm^2. In a 2-year follow-up period, cardiac death-free survival was 97.7% in the deferred group versus 94.5% in the revascularized group (P = ns), and event-free survival was 87.3% versus 80.6%, respectively (P = ns). At 2-year follow-up, only eight (4.4%) patients in the deferred group required subsequent LMCA revascularization, none of who had an MI. Thus, it is safe to defer LMCA revascularization with MLA > 6 mm^2. Additionally, the data confirms that MLA < 6.0 mm^2 is clinically significant, correlates with FFR < 0.75 (Tables 6.3 and 6.4).

More recently study with Asian populations with smaller normal coronary diameters, an MLA cut-off < 4.8 mm^2 correlates with reduced FFR < 0.8 and <4.1 mm^2 with FFR < 0.75 [22, 23].

Table 6.4 Challenges treating severely calcified coronary lesions

Respond poorly to angioplasty
Difficult to completely dilate
Prone to dissection during balloon angioplasty or predilatation
Preclude stent delivery to the desired location
Can prevent adequate stent expansion, maybe increased risk of stent thrombosis
May result in stent malapposition
Insufficient drug penetration and subsequent restenosis

6.4 Calcified Lesion

Calcium is under-recognized angiographically. In IVUS study, most of visible calcification by angiogram is correlated with arc of calcium involved, length of calcium involved, and where calcium is located [24]. So visible calcified lesion in angiography means significant calcification nearly encircled the vessel wall and spread along the vessel.

Coronary calcification has been considered a stable coronary lesion. But recent studies, however, it is not really stable because lots of microcalcification and calcified nodule had observed in unstable plaque. Patients with moderate or severe target lesion calcification (TLC) were older, had more renal insufficiency, had lower ejection fractions, and were more likely to have had a STEMI compared with patients with no or mild TLC. On the other hand, lesions with moderate or severe TLC also have other characteristics that are unfavorable, including longer lesion length, more total occlusions, more visible thrombi, and more triple-vessel disease [25].

Calcification may prevent complete expansion of the stent or interfere with stent delivery, resulting in damage either to the structure of the stent or to the polymer in the case of drug-eluting stent (DES). A malapposed, incompletely expanded, or damaged stent increases the risks for stent thrombosis of target lesion. There is general agreement that the greater the arc and length of IVUS-associated lesion calcium the greater the likelihood of underexpansion, but published or agreed criteria for recommending lesion modification prior to stent implantation does not exist. And IVUS has limitation for measure calcium thickness because of acoustic shadow, which may be an important limit to stent expansion ([26], http://www.acc.org/latest-in-cardiology/articles/2016/06/13/10/01/ivus-in-pci-guidance).

On the other hand, and most of the time, iterative IVUS imaging in conjunction with preparation and debulking of the lesion with rotational atherectomy, special balloons such as cutting or scoring and wire-cutting technique and repeated high-pressure adjunctive balloon inflations can be used to correct post-procedure stent underexpansion even in the setting of significant calcification (Fig. 6.1). Nevertheless, it is easier to prevent stent underexpansion than it is to

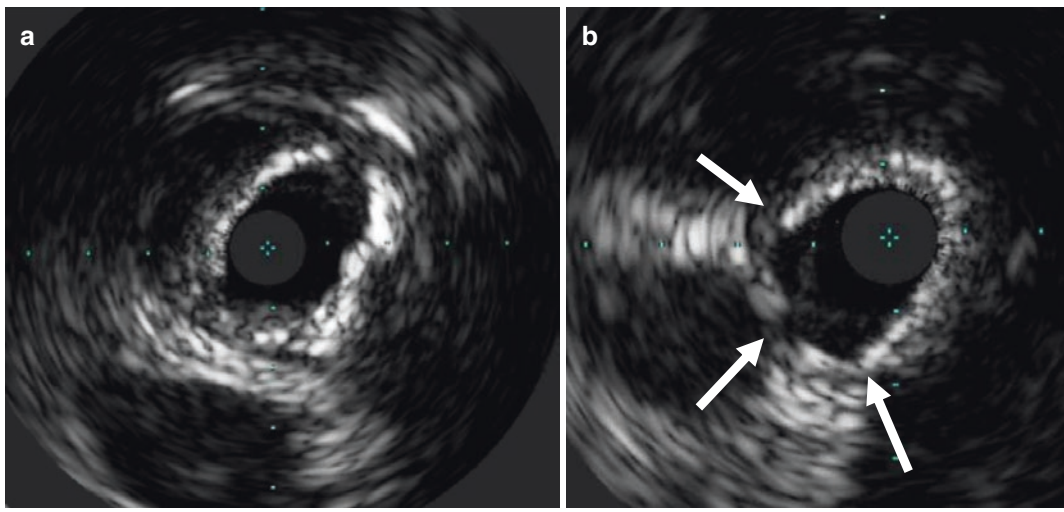

Fig. 6.1 Iterative IVUS imaging for calcified plaque at left anterior descending artery of stable angina patient. (**a**) Pre-intervention intravascular ultrasound showed superficial calcified plaque with 250° of arc. (**b**) Post-intervention intravascular ultrasound revealed luminal gain and few small cracks on superficial calcium (*white arrow*) after AngioSculpt Scout balloon® angioplasty

struggle to correct it such as stent ablation procedure. IVUS studies have shown that localized calcium deposits or the transition from calcified to non-calcified plaque (or to normal vessel wall) are foci for PCI-associated dissections. More extensive dissections occur in segments of arteries that are heavily calcified, and stent implantation into calcified lesions is more often associated with stent fracture.

6.5 Bifurcation Lesion

Coronary bifurcation PCI represents 10–15% of PCI procedures. Bifurcation lesions may show dynamic changes during PCI, with plaque/carina shift or dissection leading to side branch compromise and requiring adjustment to the interventional approach. Therefore, accurate anatomic characterization of bifurcation lesions may improve stent sizing and deployment techniques. The most important role of IVUS is correct measurement of reference vessel size of both main and side branch (SB), if operator decided to use two stent technique with proximal optimization technique.

Also IVUS can detect the distribution of plaques not only in the main branch but also in the ostium of the SB. One study revealed that SB occlusion occurred in 35% of the plaque-containing lesions at the SB ostium after PCI as compared to the 8.2% occlusion rate of plaque-free lesions at the SB ostium [27]. Therefore, wiring the SB to protect it before PCI should be considered if IVUS reveals plaque involvement at the SB ostium, but there do not appear to be reliable IVUS predictors of functional SB compromise after crossover stenting.

In IVUS study [28] regarding complex bifurcation lesions (nearly 90% of the lesions were medina class 1, 1, 1), the number of implanted stents was significantly lower in the IVUS-guided PCI group. Also, the rate of TLR was significantly lower in the IVUS-guided PCI group (6% vs 21%, $P = 0.001$). In this regard, the role of IVUS in decreasing the TLR rate may become more important, a decrease in the number of stents in the IVUS-guided PCI group may contribute to reduce the TLR rate. So, liberal and active use of IVUS in bifurcation PCI is encouraged.

6.6 Vulnerable Plaque

To Identify thrombosis or embolization-prone "vulnerable" plaques before they rupture, catheter-based intravascular imaging modalities are being developed to visualize pathologies in coronary arteries in vivo. Mounting evidences have shown three distinctive histopathological features—the presence of a thin fibrous cap (<65 μm), a lipid-rich necrotic core (>40% of total lesion area), and numerous infiltrating macrophages in the fibrous cap—are key markers of increased vulnerability in atherosclerotic plaques [29].

In the early days of coronary intervention, many coronary angiographic predictors for no-reflow or CK-MB elevation after and during PCI were identified (Table 6.5). After that to visualize these changes, the majority of catheter-based imaging modalities used IVUS with integrated tis-

Table 6.5 Predictors for no-reflow phenomenon or CK-MB elevation after or during PCI

Angiographic characteristics
Accumulated thrombus (>5 mm) proximal to the occlusion Presence of floating thrombus Persistent dye stasis distal to the obstruction Reference lumen diameter of the IRA > 4 mm
Gray scale IVUS
Large plaque burden > 70% of plaque burden Attenuated plaque Calcified nodule Intraluminal mass Soft plaque, especially lipid pool-like imaging Positive remodeling
VH-IVUS
Large necrotic core area VH-thin cap fibrous atheroma Plaque burden > 40% necrotic core > 10% of Plaque area Necrotic core contact lumen at least 3 image slices Arc of necrotic core > 36° along lumen
Spectroscopy
Max LCBI 4 mm value > 500

sue characterization techniques and OCT to enhance the characterization of vulnerable plaques.

Several studies have evaluated with IVUS to characterize morphologic predictors of plaque vulnerability, the most consistent for this phenomenon, determined by gray scale IVUS, are the presence of a large plaque burden, attenuated plaque, calcified nodule, intraluminal mass (suggestive finding for thrombus), lipid pool-like imaging, and positive vessel remodeling.

Attenuated plaque is defined as the absence of ultrasound signal behind plaque that was either hypoechoic or isoechoic to reference adventitia, but without bright calcium (Fig. 6.2). By definition, echo-attenuated plaque excludes attenuation (or, more correctly, shadowing) behind hyperechoic calcium. The hypothesis that microcalcification and thrombus with underlying advanced atherosclerosis maybe the mechanism of echo attenuation in unstable plaques. Predictors of myonecrosis during stent implantation are a large, grayscale IVUS attenuated plaque especially. When shadowing begins closer to the lumen than to the adventitia [30–32]; a large virtual histology and intravascular ultrasound (VH-IVUS) necrotic core, VH- thin-cap fibroatheroma (TCFA) [33]; a large lipid-rich plaque detected by using near infrared spectroscopy (NIRS) [34–36] (Fig. 6.3); and the presence of plaque rupture [37].

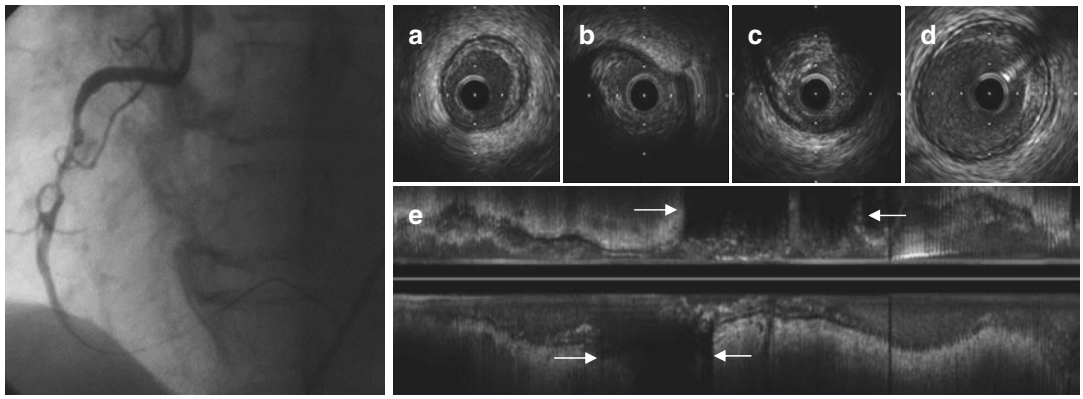

Fig. 6.2 A 75-year-old female presenting with ST elevation myocardial infarction. Pre-intervention intravascular ultrasound showed attenuated plaque (*white arrow*) on both cross-sectional (**b** and **c**) and longitudinal (**e**) intravascular ultrasound image in culprit lesion, but no echo atenuation was found on proximal (**d**) and distal (**a**) refernce segment. After stent deployment, no-reflow phenomenon was developed

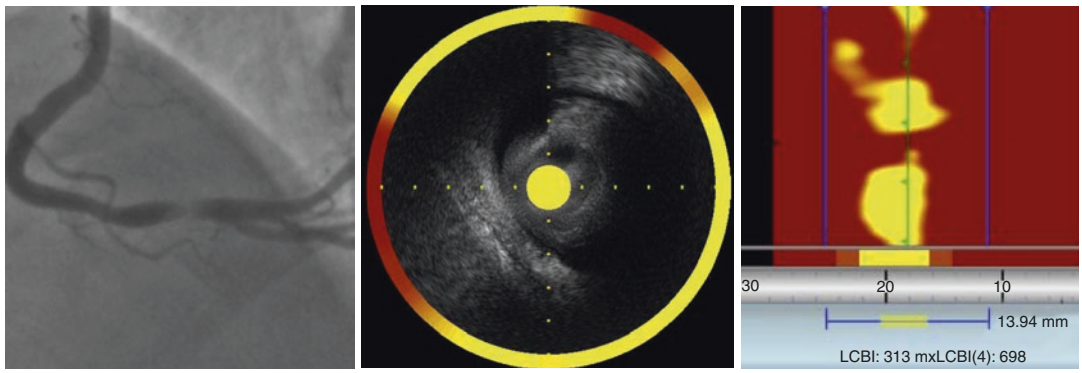

Fig. 6.3 Intravascular ultrasound for distal right coronary artery lesion of acute coronary syndrome patient showed attenuated plaque (unusual echo attenuation without calcification). Near infrared spectroscopy reveled very high maximum LCBI 4 mm value of 698

In patients with acute coronary syndrome, a calcified nodule is observed in 2–7%. IVUS characteristics of a calcified nodule were shown to be: (1) a convex shape of the luminal surface (94.1% of calcified nodules vs. 9.7% of non-nodular calcium); (2) a convex shape of the luminal side of calcium (100% vs. 16.0%); (3) an irregular luminal surface (64.7% vs. 11.6%); and (4) an irregular leading edge of calcium (88.2% vs. 19.0%) [38] (Fig. 6.4). Calcified nodules, especially close to the luminal surface of the plaque, can protrude through and rupture the fibrous cap, leading to thrombus formation and acute coronary syndromes.

However, these studies associated with gray scale IVUS for dangerous plaque are limited by their retrospective or cross-sectional design and small sample size, neither the prognostic utility (risk of future events caused by vulnerable plaques) nor the clinical utility (impact on physician decision making and/or patient outcomes) has been prospectively validated [39], and not informative about the natural history of culprit lesion formation.

More informative color-coded tissue characterization technology has been proved useful tool for TCFA imaging. Of these, VH-IVUS has correlated plaque composition with human coronary atherectomy specimens; however, considering the axial resolution of 200 μm, VH-IVUS is limited in its ability to identify TCFA. To partially overcome this limitation, the VH-TCFA definition was created [40]; VH-TCFA is defined by a focal, necrotic core-containing (10% of the total plaque area) in direct contact with the lumen at least 3 image slices, arc of NC > 36 degree along lumen and in the presence of a percent atheroma volume 40% (Fig. 6.5).

Thrombus aspiration or distal protection device deployment before PCI is recommended if

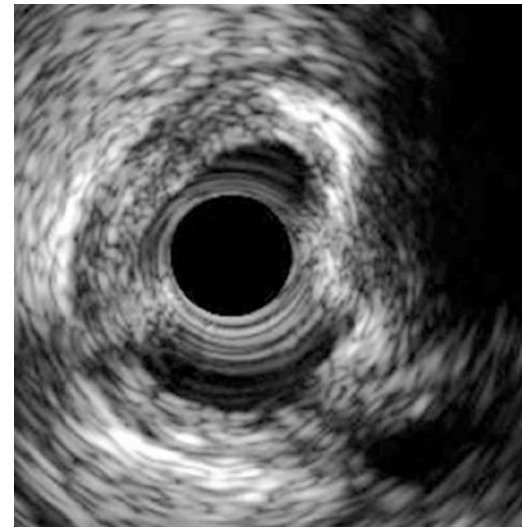

Fig. 6.4 Typical intravascular ultrasound findings of calcified nodule. (1) A convex shape of the luminal surface; (2) a convex shape of the luminal side of calcium; (3) an irregular luminal surface; and (4) an irregular leading edge of calcium

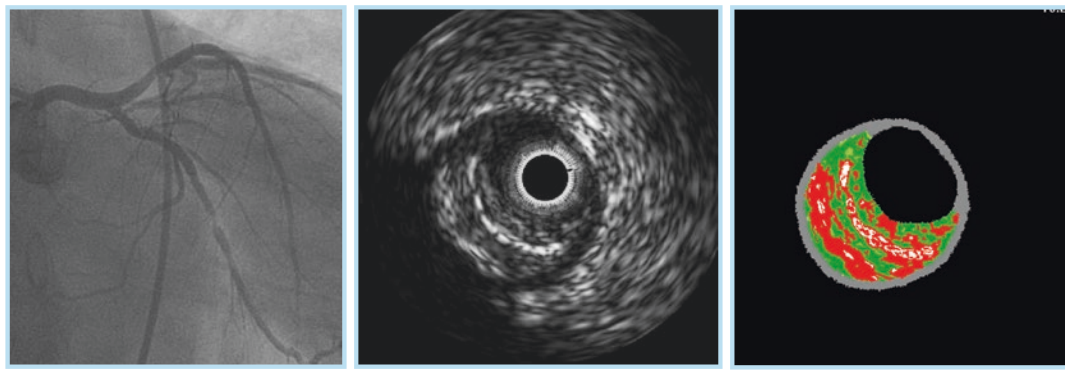

Fig. 6.5 Virtual histology and intravascular ultrasound for left circumflex lesion of acute coronary syndrome patient. (**a**) Gray scale IVUS revealed 76% plaque burden mainly soft plaque with lipid pool-like imaging. (**b**) Virtual histology showed typical findings of VH-thin cap fibroatheroma (necrotic area 49% with lumen contact)

such lesions are found. Furthermore, sometimes interventionists may encounter multiple borderline angiographic lesions without critical narrowing during acute coronary syndrome intervention. Even though inferior to OCT, IVUS as well as tissue characterization may play an important role in locating the culprit lesion where plaque rupture or TCFA has been developed [41].

To date only VH-IVUS has been shown to predict future nonculprit events. In the PROSPECT study, predictors of nonculprit events at 3 years were a VH-TCFA, an IVUS MLA < 4.0 mm^2, and an IVUS plaque burden > 70% [42]. These findings, especially the importance of a large plaque burden [37], were supported by the VIVA (VH-IVUS in Vulnerable Atherosclerosis) and ATHEROREMO-IVUS (European Collaborative Project on Inflammation and Vascular Wall Remodeling in Atherosclerosis–Intravascular Ultrasound) studies [43, 44].

PROSPECT II study is an ongoing overall prospective observational study using multimodality imaging that will examine the natural history of patients with unstable atherosclerotic coronary artery disease with IVUS and Near InfraRed Spectroscopy (NIRS), to identify plaques prone to future rupture and clinical events, plaque Burden (PB) ≥ 70% as the primary threshold defining vulnerable plaques. Currently, we cannot predict which plaques carry a risk of complications high enough to warrant prophylactic therapy, although a randomized substudy within the PROSPECT-II study will attempt to address this issue (https://clinicaltrials.gov/ct2/show/NCT02171065).

6.7 Stent Failure

Recurrence of symptoms or ischemia after PCI is the result of restenosis, incomplete initial revascularization, or disease progression. In both bare metal stents (BMS) and DES, the IVUS predictors of early stent thrombosis or in-stent restenosis (ISR) are underexpanded stent and inflow/outflow track disease (e.g., dissections, significant plaque burden, edge stenosis), but not acute stent malapposition as long as the stent is well expanded [37]. Underexpansion refers to the size of the stent, whereas malapposition refers to the contact of the stent with the vessel wall.

The use of intracoronary imaging has also been advocated in patients with stent failure, including restenosis and stent thrombosis, in order to explicate and correct underlying mechanical factors (Fig. 6.6).

6.8 Restenosis and Neoatherosclerosis

The presence of an underexpanded stent should, if possible, be corrected using repeat aggressive high-pressure noncompliant balloon angioplasty during the repeat procedure.

IVUS criteria of stent underexpansion depend on lesion location or size of reference vessel size.

Restenosis associated with stent underexpansion, repeat aggressive high-pressure balloon dilation should be used to correct underlying, stent-related, predisposing, mechanical problems revascularization and repeat PCI remains the strategy of choice for these patients if technically feasible (Table 6.6).

Recent studies have reported that one-third of patients with in-stent restenosis of bare BMS presented with acute coronary syndrome that is not regarded as clinically benign. Furthermore, both clinical and histologic studies of DES have demonstrated evidence of continuous neointimal growth during long-term follow-up, which is designated as “late catch-up” phenomenon.

In-stent neoatherosclerosis is an important substrate for late stent failure for both BMS and DES, especially in the extended phase. In light of the rapid progression in DES, early detection of neoatherosclerosis may be beneficial to improving long-term outcome of patients with DES implants [45].

Gray scale IVUS cannot discriminate neoatherosclerosis from neointimal hyperplasia. It is difficult for IVUS to determine or classify neointimal tissue because of the signal interference from metal struts, there are several reports attempting discrimination of neointimal tissues by IVUS. A case report described calcified neo-

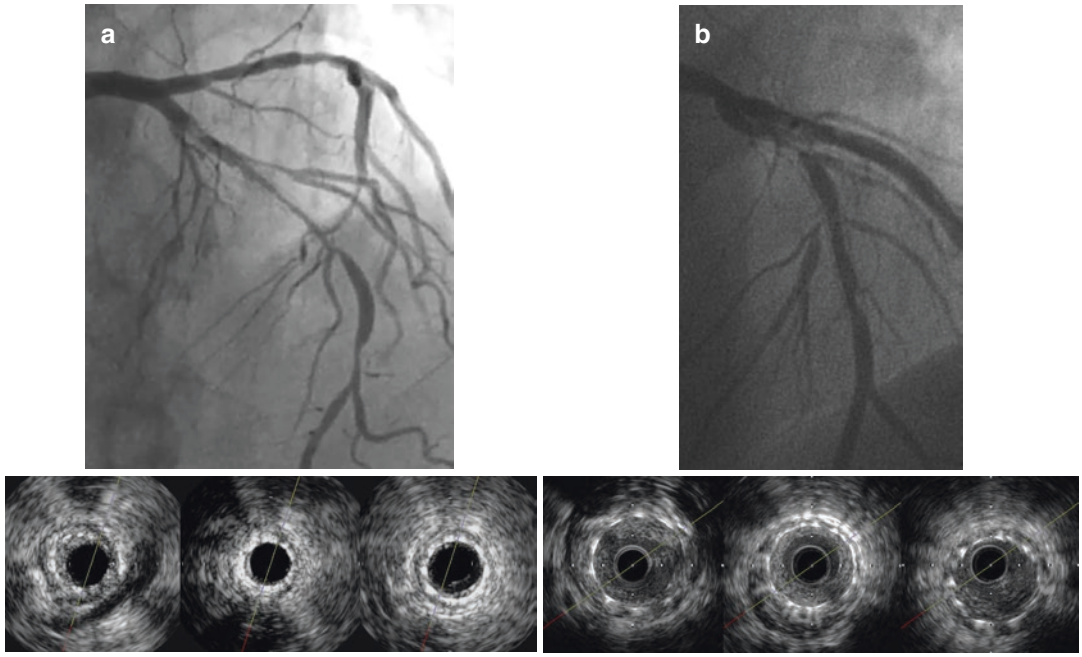

Fig. 6.6 Examples of intravascular ultrasound of in-stent restenosis. (**a**) Pre-intervention intravascular ultrasound measured minimal stent area 2.42 mm^2 for diffuse in-stent restenosis of PICO elite stent (diameter 3 mm) of mid-LAD, typical example of stent underexpansion. (**b**) Pre-intervention intravascular ultrasound measured minimal stent area 5.83 mm^2 and neointial hyperplasia area 3.84 mm^2 (65.9% of stent area) for in-stent restenosis of Endeavor stent (diameter 3 mm) of mid-LAD, typical example of intimal hyperplasia

Table 6.6 IVUS criteria of stent underexpansion and neoatherosclerosis

IVUS minimal stent area criteria of stent underexpansion
Left main above polygon of confluence <8 mm^2 in LMCA ostium or mid shaft <7 mm^2 in distal LMCA <6 mm^2 in LAD ostium <5 mm^2 in LCX ostium <5.0–5.5 mm^2 in general
In small vessel disease <80% of the average proximal and distal reference
Lumen <90% of the distal reference lumen area
VH-IVUS and NIRS findings suggest neoatherosclerosis
In-stent necrotic core and dense calcium maxLCBI 4 mm predict OCT-TCNA with a cut-off value of >144

IVUS intravascular ultrasound, *LMCA* left main coronary artery, *LAD* left anterior descending artery, *LCX* left circumflex artery, *VH-IVUS* virtual histology and intravascular ultrasound, *OCT-TCNA* OCT derived thin fibrous cap neoatheromas

intima on gray scale IVUS 8 years after BMS deployment [46], and other reports demonstrated plaque rupture and a flaplike dissection inside a restenotic stent [47, 48].

In addition, VH-IVUS has recently been reported to identify neointimal hyperplasia with unstable morphology that mimics a TCFA as in native arteries.

Using VH-IVUS, tissue characterization of restenotic in-stent neointima after DES (n = 70) and BMS (n = 47) implantation was assessed in 117 lesions with angiographic in-stent restenosis and intimal hyperplasia (IH) > 50% of the stent area. Both groups had greater percent necrotic core and percent dense calcium at maximal percent IH and maximal percent necrotic core sites, especially in stents that had been implanted for longer periods. VH-IVUS analysis showed that BMS- and DES-treated lesions develop in-stent necrotic core and dense calcium, suggesting the development of in-stent neoatherosclerosis [49] (Fig. 6.7).

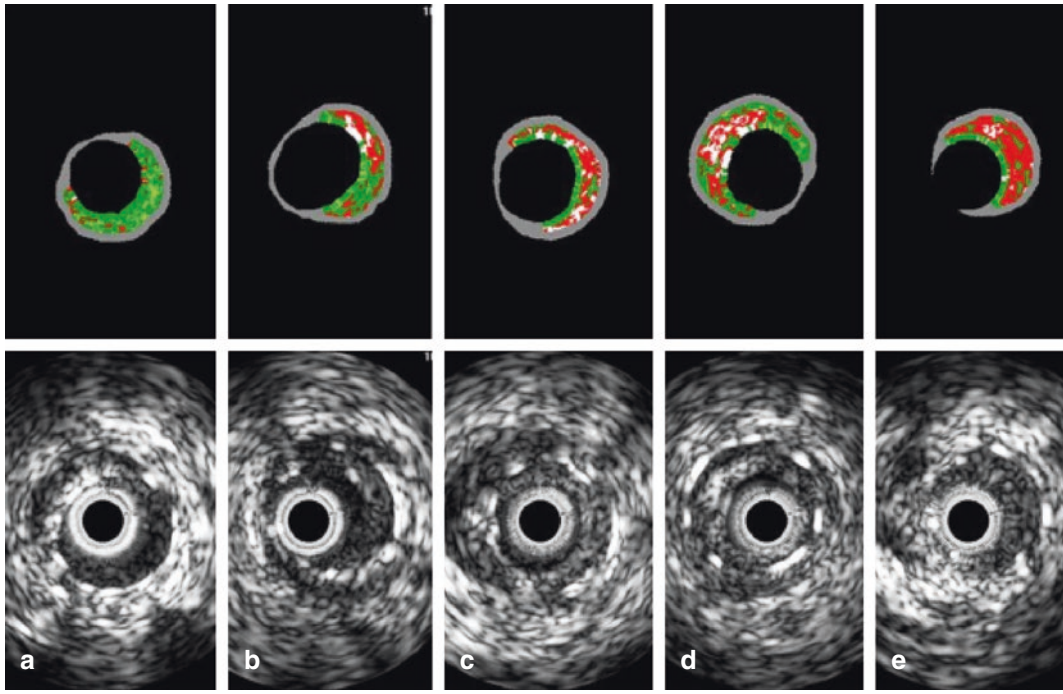

Fig. 6.7 Examples of virtual histologic intravascular ultrasound composition of the neointima at maximal percent intimal hyperplasia sites. Follow-ups of paclitaxel-eluting stent implantation at (**a**) 6 months (necrotic core 10%, dense calcium 2%), (**b**) 9 months (necrotic core 28%, dense calcium 8%), and (**c**) 22 months (necrotic core 39%, dense calcium 20%) and bare metal stent implantation at (**d**) 48 months (necrotic core 40%, dense calcium 25%) and (**e**) 57 months (necrotic core 57%, dense calcium 15%) (Kang et al. Am J Cardiol 2010;106:1561–1565)

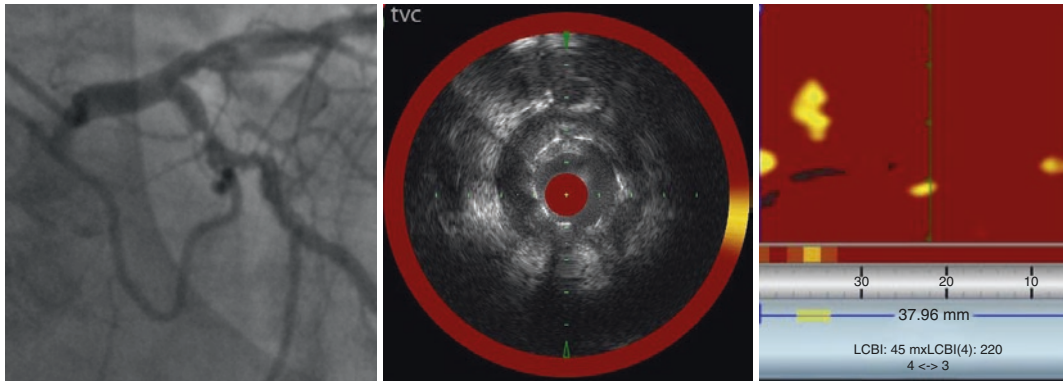

Fig. 6.8 IVUS for LCX ISR lesion showed modest intima hyperplasia and stent fracture. Near infrared spectroscopy revealed maximum LCBI 4 mm value of 220, suggested presence of thin fibrous cap neoatheromas

Recent study evaluated ability of NIRS to detect OCT derived thin fibrous cap neoatheromas [TCNA; thin fibrous cap covering the lipid core (<65 μm)] are prone to rupture and higher risk of late stent failure. In 39 drug-eluting stents with ISR, values of LCBI derived by NIRS were compared with the OCT-derived thickness of the fibrous cap covering neoatherosclerotic lesions. A total of 22 (49%) in-stent neointimas were identified as lipid rich by both NIRS and

OCT. There was good agreement between OCT and NIRS in identifying lipid within in-stent neointima. OCT identified TCNA in 12 stents (23%), the minimal cap thickness of in-stent neoatherosclerotic plaque measured by OCT correlated with the maxLCBI 4mm (maximal LCBI per 4 mm) within the stent ($r = -0.77$, $P < 0.01$). Moreover, maxLCBI 4 mm was able to accurately predict TCNA with a cut-off value of >144. NIRS correlates with OCT identification of lipids in stented vessels and is able to predict the presence of thin fibrous cap neoatheroma [50] (Fig. 6.8).

References

1. Levine GN, Bates ER, Blankenship JC, Bailey SR, Bittl JA, Cercek B, Chambers CE, Ellis SG, Guyton RA, Hollenberg SM, Khot UN, Lange RA, Mauri L, Mehran R, Moussa ID, Mukherjee D, Nallamothu BK, Ting HH, American College of Cardiology Foundation, American Heart Association Task Force on Practice Guidelines, Society for Cardiovascular Angiography and Interventions. 2011 ACCF/AHA/SCAI guideline for percutaneous coronary intervention. A report of the American College of Cardiology Foundation/American Heart Association Task Force on Practice Guidelines and the Society for Cardiovascular Angiography and Interventions. J Am Coll Cardiol. 2011;58:44–122.
2. Authors/Task Force Members, Windecker S, Kolh P, Alfonso F, Collet JP, Cremer J, Falk V, Filippatos G, Hamm C, Head SJ, Jüni P, Kappetein AP, Kastrati A, Knuuti J, Landmesser U, Laufer G, Neumann FJ, Richter DJ, Schauerte P, Sousa Uva M, Stefanini GG, Taggart DP, Torracca L, Valgimigli M, Wijns W, Witkowski A. 2014 ESC/EACTS guidelines on myocardial revascularization: the Task Force on Myocardial Revascularization of the European Society of Cardiology (ESC) and the European Association for Cardio-Thoracic Surgery (EACTS)Developed with the special contribution of the European Association of Percutaneous Cardiovascular Interventions (EAPCI). Eur Heart J. 2014;35:2541–619.
3. Pijls NH, Sels JW. Functional measurement of coronary stenosis. J Am Coll Cardiol. 2012;59:1045–57.
4. Takagi A, Tsurumi Y, Ishii Y, et al. Clinical potential of intravascular ultrasound for physiological assessment of coronary stenosis: relationship between quantitative ultrasound tomography and pressure-derived fractional flow reserve. Circulation. 1999;100:250–5.
5. Briguori C, Anzuini A, Airoldi F, et al. Intravascular ultrasound criteria for the assessment of the functional significance of intermediate coronary artery stenoses and comparison with fractional flow reserve. Am J Cardiol. 2001;87:136–41.
6. Lee CH, Tai BC, Soon CY, et al. New set of intravascular ultrasound-derived anatomic criteria for defining functionally significant stenoses in small coronary arteries (results from intravascular ultrasound diagnostic evaluation of atherosclerosis in Singapore [IDEAS] study). Am J Cardiol. 2010;105:1378–84.
7. Kang SJ, Lee JY, Ahn JM, et al. Validation of intravascular ultrasound-derived parameters with fractional flow reserve for assessment of coronary stenosis severity. Circ Cardiovasc Interv. 2011;4:65–71.
8. Kang SJ, Ahn JM, Song H, et al. Usefulness of minimal luminal coronary area determined by intravascular ultrasound to predict functional significance in stable and unstable angina pectoris. Am J Cardiol. 2012;109:947–53.
9. Ben-Dor I, Torguson R, Gaglia MA Jr, et al. Correlation between fractional flow reserve and intravascular ultrasound lumen area in intermediate coronary artery stenosis. EuroIntervention. 2011;7:225–33.
10. Ben-Dor I, Torguson R, Deksissa T, et al. Intravascular ultrasound lumen area parameters for assessment of physiological ischemia by fractional flow reserve in intermediate coronary artery stenosis. Cardiovasc Revasc Med. 2012;13:177–82.
11. Koo BK, Yang HM, Doh JH, et al. Optimal intravascular ultrasound criteria and their accuracy for defining the functional significance of intermediate coronary stenoses of different locations. J Am Coll Cardiol Intv. 2011;4:803–11.
12. Waksman R, Legutko J, Singh J, et al. FIRST: fractional flow reserve and intravascular ultrasound relationship study. J Am Coll Cardiol. 2013;61:917–23.
13. Stone GW. VERDICT/FIRST: prospective, multicenter study examining the correlation between IVUS and FFR parameters in intermediate lesions. Available at https://www.tctmd.com/slide/verdictfirst-prospective-multicenter-study-examining-correlation-between-ivus-and-ffr. 2013.
14. Kang SJ, Ahn JM, Han S, et al. Sex differences in the visual-functional mismatch between coronary angiography or intravascular ultrasound versus fractional flow reserve. J Am Coll Cardiol Intv. 2013;6:562–8.
15. Abizaid A, Mintz GS, Pichard AD, Kent KM, Satler LF, Walsh CL, Popma JJ, Leon MB. Clinical, intravascular ultrasound, and quantitative angiographic determinants of the coronary flow reserve before and after percutaneous transluminal coronary angioplasty. Am J Cardiol. 1998;82:423–8.
16. Nishioka T, Amanullah AM, Luo H, Berglund H, Kim CJ, et al. Clinical validation of intravascular ultrasound imaging for assessment of coronary stenosis severity: comparison with stress myocardial perfusion imaging. J Am Coll Cardiol. 1999;33:1870–8.
17. Abizaid AS, Mintz GS, Mehran R, Abizaid A, Lansky AJ, et al. Long-term follow-up after percutaneous transluminal coronary angioplasty was not performed based on intravascular ultrasound findings:

importance of lumen dimensions. Circulation. 1999;100:256–61.
18. Lotfi A, Jeremias A, Fearon WF, Feldman MD, Mehran R, Messenger JC, Grines CL, Dean LS, Kern MJ, Klein LW, Society of Cardiovascular Angiography and Interventions. Expert consensus statement on the use of fractional flow reserve, intravascular ultrasound, and optical coherence tomography: a consensus statement of the Society of Cardiovascular Angiography and Interventions. Catheter Cardiovasc Interv. 2014;83(4):509–18.
19. Sano K, Mintz GS, Carlier SG, de Ribamar Costa J Jr, Qian J, Missel E, Shan S, Franklin-Bond T, Boland P, Weisz G, Moussa I, Dangas GD, Mehran R, Lansky AJ, Kreps EM, Collins MB, Stone GW, Leon MB, Moses JW. Assessing intermediate left main coronary lesions using intravascular ultrasound. Am Heart J. 2007;154:983–8.
20. Jasti V, Ivan E, Yalamanchili V, Wongpraparut N, Leesar MA. Correlations between fractional flow reserve and intravascular ultrasound in patients with an ambiguous left main coronary artery stenosis. Circulation. 2004;110:2831–6.
21. de la Torre Hernandez JM, Hernandez Hernandez F, Alfonso F, Rumoroso JR, Lopez-Palop R, et al. Prospective application of pre-defined intravascular ultrasound criteria for assessment of intermediate left main coronary artery lesions results from the multicenter LITRO study. J Am Coll Cardiol. 2011;58:351–8.
22. Park SJ, Ahn JM, Kang SJ, et al. Intravascular ultrasound-derived minimal lumen area criteria for functionally significant left main coronary artery stenosis. JACC Cardiovasc Interv. 2014;7:868–74.
23. Kang SJ, Lee JY, Ahn JM, Song HG, Kim WJ, et al. Intravascular ultrasound-derived predictors for fractional flow reserve in intermediate left main disease. JACC Cardiovasc Interv. 2011;4:1168–74.
24. Mintz GS, Popma JJ, Pichard AD, Kent KM, Satler LF, Chuang YC, Ditrano CJ, Leon MB. Patterns of calcification in coronary artery disease. A statistical analysis of intravascular ultrasound and coronary angiography in 1155 lesions. Circulation. 1995;91:1959–65.
25. Généreux P, Madhavan MV, Mintz GS, Maehara A, Palmerini T, Lasalle L, Xu K, McAndrew T, Kirtane A, Lansky AJ, Brener SJ, Mehran R, Stone GW. Ischemic outcomes after coronary intervention of calcified vessels in acute coronary syndromes. Pooled analysis from the HORIZONS-AMI (harmonizing outcomes with revascularization and stents in acute myocardial infarction) and ACUITY (acute catheterization and urgent intervention triage strategy) TRIALS. J Am Coll Cardiol. 2014;63:1845–54.
26. Mintz GS. Intravascular imaging of coronary calcification and its clinical implications. JACC Cardiovasc Imaging. 2015;8:461–7.
27. Furukawa E, Hibi K, Kosuge M, et al. Intravascular ultrasound predictors of side branch occlusion in bifurcation lesions after percutaneous coronary intervention. Circ J. 2005;69:325–30.
28. Patel Y, Depta JP, Novak E, et al. Long-term outcomes with use of intravascular ultrasound for the treatment of coronary bifurcation lesions. Am J Cardiol. 2012;109:960–5.
29. Virmani R, Burke AP, Farb A, Kolodgie FD. Pathology of the vulnerable plaque. J Am Coll Cardiol. 2006;47:13–8.
30. Lee SY, Mintz GS, Kim SY, et al. Attenuated plaque detected by intravascular ultrasound: clinical, angiographic, and morphologic features and post-percutaneous coronary intervention complications in patients with acute coronary syndromes. J Am Coll Cardiol Intv. 2009;2:65–72.
31. Wu X, Mintz GS, Xu K, et al. The relationship between attenuated plaque identified by intravascular ultrasound and no-reflow after stenting in acute myocardial infarction: the HORIZONS-AMI (harmonizing outcomes with revascularization and stents in acute myocardial infarction) trial. J Am Coll Cardiol Intv. 2011;4:495–502.
32. Shiono Y, Kubo T, Tanaka A, et al. Impact of attenuated plaque as detected by intravascular ultrasound on the occurrence of microvascular obstruction after percutaneous coronary intervention in patients with ST-segment elevation myocardial infarction. J Am Coll Cardiol Intv. 2013;6:847–53.
33. Claessen BE, Maehara A, Fahy M, Xu K, Stone GW, Mintz GS. Plaque composition by intravascular ultrasound and distal embolization after percutaneous coronary intervention. J Am Coll Cardiol Img. 2012;5:S111–8.
34. Goldstein JA, Maini B, Dixon SR, et al. Detection of lipid-core plaques by intracoronary near-infrared spectroscopy identifies high risk of periprocedural myocardial infarction. Circ Cardiovasc Interv. 2011;4:429–37.
35. Raghunathan D, Abdel-Karim AR, Papayannis AC, et al. Relation between the presence and extent of coronary lipid core plaques detected by near-infrared spectroscopy with postpercutaneous coronary intervention myocardial infarction. Am J Cardiol. 2011;107:1613–8.
36. Brilakis ES, Abdel-Karim AR, Papayannis AC, et al. Embolic protection device utilization during stenting of native coronary artery lesions with large lipid core plaques as detected by nearinfrared spectroscopy. Catheter Cardiovasc Interv. 2012;80:1157–62.
37. Mintz GS. Clinical utility of intravascular imaging and physiology in coronary artery disease. J Am Coll Cardiol. 2014;64:207–22.
38. Lee JB, Mintz GS, Lisauskas JB, et al. Histopathologic validation of the intravascular ultrasound diagnosis of calcified coronary artery nodules. Am J Cardiol. 2011;108:1547–51.
39. Alsheikh-Ali AA, Kitsios GD, Balk EM, Lau J, Ip S. The vulnerable atherosclerotic plaque: scope of the literature. Ann Intern Med. 2010;153:387–95.

40. Rodriguez-Granillo GA, Garcia-Garcia HM, McFadden EP, Valgimigli M, Aoki J, de Feyter P, Serruys PW. In vivo intravascular ultrasoundderived thin-cap fibroatheroma detection using ultrasound radiofrequency data analysis. J Am Coll Cardiol. 2005;46:2038–42.
41. Wu X, Maehara A, Mintz GS, et al. Virtual histology intravascular ultrasound analysis of non-culprit attenuated plaques detected by grayscale intravascular ultrasound in patients with acute coronary syndromes. Am J Cardiol. 2010;105:48–53.
42. Stone GW, Maehara A, Lansky AJ, et al. A prospective natural-history study of coronary atherosclerosis. N Engl J Med. 2011;364:226–35.
43. Calvert PA, Obaid DR, O'Sullivan M, et al. Association between IVUS findings and adverse outcomes in patients with coronary artery disease: the VIVA (VH-IVUS in vulnerable atherosclerosis) study. JACC Cardiovasc Imaging. 2011;4:894–901.
44. Cheng JM, Garcia-Garcia HM, de Boer SP, et al. In vivo detection of high-risk coronary plaques by radiofrequency intravascular ultrasound and cardiovascular outcome: results of the ATHEROREMO-IVUS study. Eur Heart J. 2014;35:639–47.
45. Park SJ, Kang SJ, Virmani R, Nakano M, Ueda Y. In-stent neoatherosclerosis: a final common pathway of late stent failure. J Am Coll Cardiol. 2012;59:2051–7.
46. Appleby CE, Bui S, Dzavı'k V. A calcified neointima-"stent" within a stent. J Invasive Cardiol 2009;21:141–143.
47. Fineschi M, Carrera A, Gori T. Atheromatous degeneration of the neointima in a bare metal stent: intravascular ultrasound evidence. J Cardiovasc Med. 2009;10:572–3.
48. Hoole SP, Starovoytov A, Hamburger JN. In-stent restenotic lesions can rupture: a case against plaque sealing. Catheter Cardiovasc Interv. 2010;77:841–2.
49. Kang SJ, Mintz GS, Park DW, Lee SW, Kim YH, Lee CW, Han KH, Kim JJ, Park SW, Park SJ. Tissue characterization of in-stent neointima using intravascular ultrasound radiofrequency data analysis. Am J Cardiol. 2010;106:1561–5.
50. Roleder T, Karimi Galougahi K, Chin CY, Bhatti NK, Brilakis E, Nazif TM, Kirtane AJ, Karmpaliotis D, Wojakowski W, Leon MB, Mintz GS, Maehara A, Stone GW, Ali ZA. Utility of near-infrared spectroscopy for detection of thin-cap neoatherosclerosis. Eur Heart J Cardiovasc Imaging. 2017;18:663. doi:10.1093/ehjci/jew198.